JOURNAL OF Applied Polymer SCIENCE

Characterization of the Draping Behavior of Jute Woven Fabrics for Applications of Natural-Fiber/Epoxy Composites

Ahmed El-Sabbagh,[1,2] Iman Taha[2]

[1]Institute for Polymer Materials and Plastics Processing, Clausthal University of Technology, Agricolastrasse 6, 38678 Clausthal-Zellerfeld, Germany

[2]Design and Production Engineering Department, Ain Shams University, El-Sarayat Strasse 1, Abbassia, Cairo, Egypt

Correspondence to: A. El-Sabbagh (E-mail: ahmed.sabbagh@tu-clausthal.de)

ABSTRACT: In this study, we investigated the draping behavior of jute woven fabric to study the feasibility of using natural fabrics in place of synthetic glass-fiber fabrics. Draping behavior describes the in-mold deformation of fabrics, which is vital for the end appearance and performance of polymer composites. The draping coefficient was determined with a common drapemeter for fabrics with densities of 228–765 g/m^2 and thread counts under different humidity and static dynamic conditions. The results were compared to glass-fiber fabrics with close areal densities. Characterization of the jute fabrics was carried out to fill the knowledge gap about natural-fiber fabrics and to ease their modeling. The tensile and bending stiffnesses and the shear coupling were also characterized for a plain woven jute fabric with a tensile machine, Shirley bending tester, and picture frame, respectively. As a case study, the draping and resin-transfer molding of the jute fabric over a complex asymmetric form was performed to measure the geometrical conformance. The adoption of natural fibers as a substitute for synthetic fibers, where the strength requirements are satisfied, would thus require no special considerations for tool design or common practices. However, the use of natural fibers would lead to weight and cost reductions. © 2013 Wiley Periodicals, Inc. J. Appl. Polym. Sci. 130: 1453–1465, 2013

KEYWORDS: biomaterials; composites; molding; theory and modeling

Received 6 February 2013; accepted 14 March 2013; Published online 26 April 2013

DOI: 10.1002/app.39261

INTRODUCTION

Natural Fibers as New Materials

The use of natural fibers has found increased interest in the last decade, especially in the field of fiber-reinforced polymer composites. In addition to their availability from renewable resources and their low cost, natural fibers offer further advantages over synthetic fibers, including a low density (1.4 vs 2.5 g/cm^3 for glass fibers; this leads to a 45% weight reduction), biodegradability, less wear during processing, and low energy consumption.[1–3]

As for fiber reinforcements, natural fibers, such as sisal, jute, and date palm fibers,[3–5] have proven to contribute to the strengthening of polymer composites. Intensive research has been conducted on the use of natural-fiber/polymer composites for thermoplastic matrix extrudates and injection-molded parts.[6,7] However, large-area components are mostly manufactured by hand layup,[8,9] press-molding,[10] or resin-transfer molding techniques.[11] In addition to the fiber permeability, wettability, and resin absorption, the draping behavior of woven and nonwoven fabrics plays a vital role in aesthetics and the realization of the final construction. It is thus often of great interest to investigate the draping behavior of fabrics in use before the manufacturing step to prevent wrinkling at deformation points and ensure the dimensional accuracy.

Draping Measuring

According to Collier,[12] *draping* is defined as a fabric's ability to form folds when it is bent under its own weight. The draping behavior of fabrics was subjectively evaluated by a panel of judges in the early days. Structured objective investigations of fabric draping behavior can be traced back to a classic article authored by Peirce in 1930,[13] as quoted by Kenkare and May-Plumlee.[14] Peirce[13] developed the cantilever method (commercially known as the Shirley Stiffness Tester) to measure a fabric's bending properties and then used the dimensional bending characteristics as a measure of drape.

Previous research has focused further on the development of direct quantitative evaluation methods to determine the drape and the correlation of these drape values with measured fabric properties thought to influence drape, such as fabric bending and shearing properties in addition to weight and thickness.

However, the characterization of the drape with a two-dimensional measurement imposes many limitations on describing the complex, anisotropic behavior of fabrics. To overcome these problems, the Fabric Research Laboratories (FRL) developed the FRL drapemeter,[15] as discussed in ref. 14, to measure the drape in three dimensions. Collier[12] described a static drape tester that has often been used in research and that requires the placement of a circular fabric specimen between two smaller circular plates, which are supported above the base of the instrument. The annular ring of fabric not held between the plates is free to drape over the edge of the support. Paper tracings of draped patterns were obtained and compared to undraped patterns to determine a drape coefficient (DC). Collier[12] further developed this method such that the drape tester uses a bottom surface of photovoltaic cells to determine the amount of blocked light being absorbed by the photovoltaic cells, and this is related to the amount of drape of the fabric specimen.

To minimize the tediousness and error of the FRL method, Kenkare and May-Plumlee[14] proposed the further measurement of three-dimensional draping with digital technology. Here, a digital image of each draped sample is captured and further processed with Adobe Photoshop software to determine the drape coefficient, which is defined as follows:

$$DC = \frac{\text{Area under the draped sample} - \text{Area of the underlying disc}}{\text{Area of the specimen} - \text{Area of the underlying disc}} \quad (1)$$

Draping Description Mechanisms

In recent years, the previous understanding of a fabric's deformation mechanisms has further been incorporated into computer simulations. The simulations start with the component's surface geometry and generally assume an initially orthogonal net. An initial point of contact is specified, and an initial warp and weft yarn path is generated from the start point over the surface. The woven cloth is then modeled as a net made up of equally sided cells corresponding to a free linkage of four bars of equal length defined by the warp and weft yarns and constrained by the initial warp and weft yarns. The surface is then covered in an iterative process, which brings the cell edges into contact with the surface.[16] This is a typical kinematic solution for a draping problem where the bending and shear stiffnesses are neglected and only the intraply shear (trellis) is considered. This type of solution is considered an approximation and suits the hand-layup processes and not automated ones.[17] This kinematic solution predicts the wrinkling formation onset; a threshold lock angle is reached upon fiber buckling (out-of-plane deformation). A more realistic solution deals with the global deformation, where the fabric in-plane tensile properties and bending out-of-plane stiffness are considered.[17] This solution can deal with the different weaving structures of the fabric textile. The boundary conditions of the blank holder and the underlying die and consequently the contact friction coefficient are also considered. The interply shear between the layers of the fabrics are also considered. Boisse et al.[18] reported more decisively that there was no direct relation between the shear angle and the out-of-plane deformation (wrinkling). Wrinkling takes place essentially by a whole system of strains, stiffnesses, and boundary conditions. The bending stiffness plays a major role in determining the shape of these wrinkles.

The modeling of the draping behavior requires the characterization of the textile tensile and bending stiffnesses in the warp and weft directions, in-plane shear, lock angle, compaction, and interply friction. For the kinematic model, one needs only to define the lock angle and the fabric compression behavior in terms of the stress–strain or pressure–fiber volume fraction. Therefore, it is necessary to define these modeling parameters for new fabric materials such as jute fabrics.

Fong et al.[19] investigated not only the material effect but also the role of the draping behavior during the manufacturing processes, especially for resin-transfer molding techniques. It has been shown that the drape of fabrics causes the fiber orientation to change and the fiber volume fraction to be inhomogeneous throughout the composite.[19] According to Hancock and Potter,[16] these problems become even more apparent when one deals with unidirectional fabric or natural fibers, which are characterized by both macroflows and microflows[20] (flow through the pores and flow within the fibers, respectively).

Although the specific properties of natural fibers are acceptable compared to those of glass fibers, drapability characteristics are rare,[21] and hence, designers tend not to use material with unexpected deformation behaviors. A solution to this is offered here in a systematic characterization study of the DCs of selected natural fibers. A case study is given to ensure the feasibility of the natural fibers as potential competitors for synthetic ones. The objectives of this study were as follows:

- To characterize the jute-fabric properties, especially those related to draping, and to compare them with those of a matching/similar glass-fiber fabric.
- To test the modeling techniques and determine how it is possible to predict wrinkle formation and to compare the modeled results with those of an experimental trial.

EXPERIMENTAL

Materials

Two suppliers of jute fibers were used in this investigation. Three types of jute-fiber wovens (jute fibre Egypt (JFE)) were supplied by Al-Sharqeya for Jute Productions (Belbeis, Egypt). Jute fibers in the form of a woven fabric, provided by Jute and More (Augsburg, Germany) and of Bangladeshi origin, were also considered (jute fibre Germany (JFG)). Glass fibers supplied by HP Textiles were examined for comparative analysis. The nomenclature of the fabrics is given in Table I.

Characterization of the Natural Fabrics

Physical Properties. Physical characterization tests were required for the jute woven fabrics because of a lack of knowledge of these products' properties in addition to the generally known inconsistency of production. A knowledge of the physical properties is vital for an analysis and interpretation of the draping behavior of woven fabrics, especially in cases where nonsymmetric draping is observed along the orthogonal warp and weft directions.

The fiber diameters were measured with a Helmut Hund GmbH trinocular microscope at 40× magnification. Ten measurements were taken in each weft and warp direction. The average values for each fiber type were then determined. The linear

Table I. Nomenclature of the Fabrics under Investigation

Nomenclature	Fabric origin	Description
JFEN 1 × 1	Al-Sharqeya for Jute Productions	Egyptian woven textile with one thin fibers in both weft and warp directions
JFEN 2 × 1	Al-Sharqeya for Jute Productions	Egyptian woven textile with two thin fibers in the weft and one thin fiber in the weft direction
JFEK 1 × 1	Al-Sharqeya for Jute Productions	Egyptian woven textile with one thick fiber in the weft and one thin fiber in the warp direction
JFGN 1 × 1	Jute and More	German woven textile with one thin fibers in both weft and warp directions
GF210	HP Textiles	Close planar density to JFEN 1 × 1 for the sake of comparison
GF390	HP Textiles	Close planar density to JFGN 1 × 1 for the sake of comparison

density in terms of Tex number (grams per 1000 meters) was measured for the various fiber types. Single fibers 50 cm in length were weighed on a digital balance, and the weight per unit length was calculated. The planar density was determined for 30-cm^2 pieces of fabric.

Chemical Analysis. Fourier transformation infrared (FTIR) analysis allows one to identify the characteristic molecules of chemical substances. This method is found to be very beneficial for the characterization of natural fibers and the identification of any structural changes occurring because of chemical modification processes. This test is carried out to check whether there is a significant difference between the two fabric supplies with regard to chemical treatments. FTIR spectroscopy was carried out on the investigated fibers with a Stepscan FTIR FTS 7000 spectrometer over a wave-number range of 4000–400 cm^{-1}.

Mechanical Testing. Single yarns were extracted from each fabric in both the weft and warp directions and were tested for tensile strength and stiffness according to DIN EN 13895-1:2003 (D), with a free gauge length of 500 ± 1 mm tensioned at a constant speed of 500 mm/min.

Similarly, woven fabric was tested according to DIN EN ISO 13934-1:1999, where the sample dimensions allowed for a free gauge length equal to 200 mm at a width of 50 ± 0.5 mm^2 without fringes. The test speed was set at 20 mm/min. All of the tension tests were performed on a 2-kN Zwick Roell universal testing machine. Tensile testing of the fabric defined the tensile stiffnesses in the warp and weft directions (E_1 and E_2, respectively).

Drapability Tests. ***Drapemeter testing.*** The drapability describes the extent to which a fabric will deform when it is allowed to hang under its own weight. This can be described in terms of the so-called DC, which is generally defined as a ratio between the deformed and undeformed fabric as described earlier. Greater values of DC indicated that the fabric is made of a stiff material. The characterization of DC is not sufficient to describe the draping of a fabric. The number of folds and their wavelength, distribution, and amplitude are all needed to characterize the draping behavior.[22] However, this test helps to provide a good prediction of the behavior of the fabric. To model the fabric draping, some properties should be identified, namely, the stiffness moduli in both the warp and weft directions.

Figure 1 shows the test rig, composed of an 18-cm circular disc, over which circular fabric samples of 30 and 36 cm, respectively, were placed and left to bend under their own weights [Figure

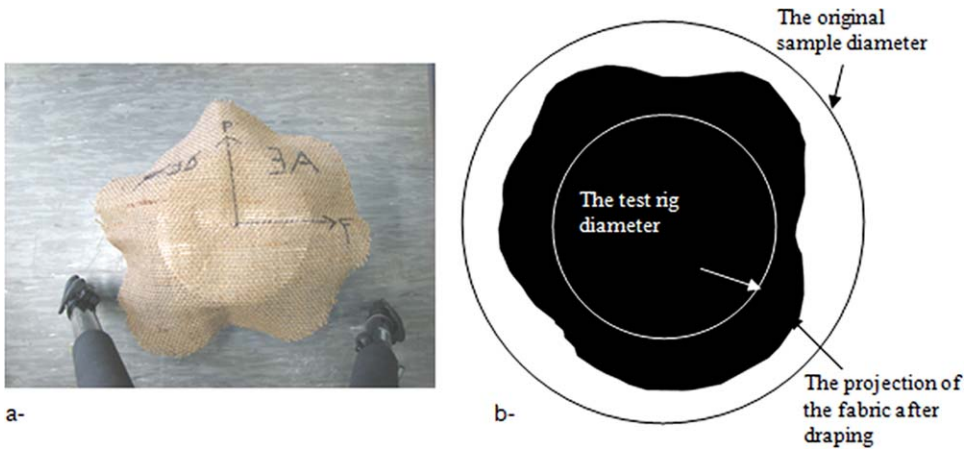

Figure 1. (a) Draped sample and (b) image processing of the captured image. [Color figure can be viewed in the online issue, which is available at wileyonlinelibrary.com.]

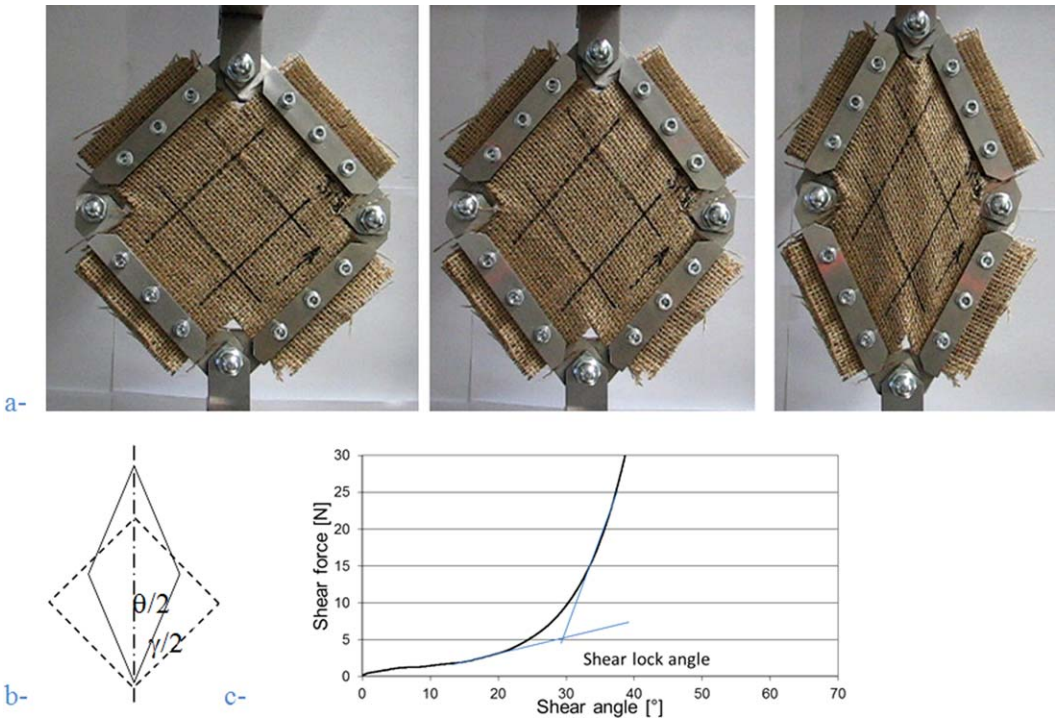

Figure 2. Picture frame test showing the (a) shearing of the jute fabric until wrinkle formation (displacement–force), which was converted to a shear strain–shear stress relation, (b) frame angle change during testing, and (c) lock angle definition. [Color figure can be viewed in the online issue, which is available at wileyonlinelibrary.com.]

1(a)]. The test setup was composed of a digital camera placed on a tripod at a constant vertical distance of 62.5 cm from the upper test rig surface.

An image of the draped fabric was shot with the camera with a monocolor background (to help with contrast) and at a predefined resolution of 2048 × 1568 pixels. Image transfer to a PC allowed us to use simple image processing programs for the manual definition (redrawing) of the draped fabric contour. In this case, the simple Microsoft Paint was used to define and fill out the contours, as depicted in Figure 1(b). The image was then further processed on a PC to determine the area after deformation and relate it to the initial area. The picture was first converted into a binary image (black and white), where it could be recognized by MATLAB. A code written to calculate the black area was applied for each picture on the basis of the calculated relation between the captured image distance and the actual area per digital pixel, as given by the following:[14]

$$\mathrm{DC} = \frac{\text{Image [pixels/(pixels/cm}^2\text{)]-Area of the underlying disc (cm}^2\text{)}}{\text{Area of the specimen (cm}^2\text{)-Area of the underlying disc (cm}^2\text{)}} \quad (2)$$

Each sample was tested three times for each face. The upper and lower fabric faces of the fabric were named a and b, respectively.

We investigated the effect of the humidity on the draping behavior by preparing samples under a dry atmosphere (with oven drying at 110°C until a stagnant weight was reached) and an ambient humid atmosphere with 65% relative humidity [RH; conditioning under 65% for 24 h]. Only jute fabrics were exposed to RH conditions to monitor the humidity effect on the hydrophilic fibers.

The dynamic DC was determined as the change in DC with respect to time. This test was performed for fabrics 36 cm in diameter, where the digital images were captured in 1-, 2-, 5-, 10-, 30-, and 60-min intervals and were further processed as described previously to determine a time-dependent DC. The measured DC/time relationship in this work is not to be confused with the *dynamic drape*, which is defined as the change in the draping shape of fabrics under the influence of a swinging motion.[14]

Shirley stiffness testing. This test was carried out to define the bending moduli of the fabric in both the warp and weft directions according to ASTM D 1388-96. A sample 25 mm in breadth and 300 mm in length along the tested fabric direction was used. The fabric was moved on an inclination of 41.5 ± 0.5° below the plane of the platform surface until the overhanging fabric touched the inclined indicator surface. The bending stiffness was defined with eqs. (3) and (4):

$$\text{Flexural rigidity} = \text{Fabric areal density} \times (\text{Bending length})^3 \quad (3)$$

$$\text{Bending modulus} = 12 \times \text{Flexural rigidity}/\text{Thickness}^3 \quad (4)$$

Picture frame testing. We implemented an in-plane shear to characterize the shear coupling (G) value. The test was

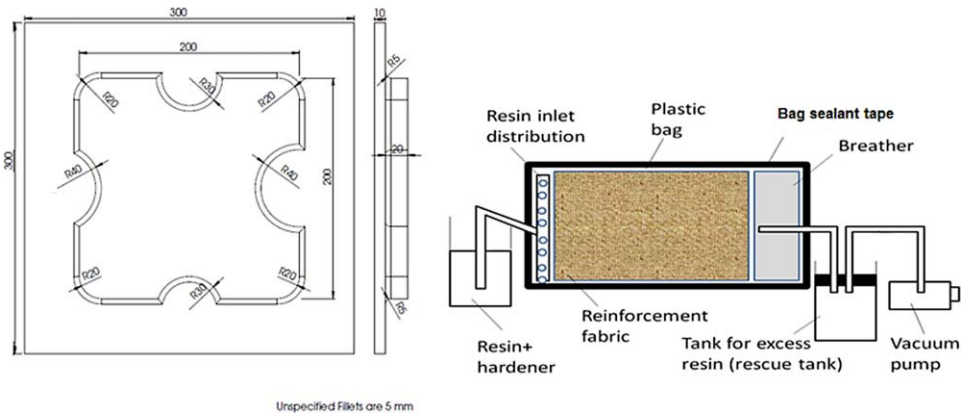

Figure 3. Asymmetric form used to evaluate the jute fabric drapability: (a) constructional drawing and (b) schematic drawing of a simplified VARI process. BST: Bag sealant tape. [Color figure can be viewed in the online issue, which is available at wileyonlinelibrary.com.]

performed on a Zwick 2-kN load cell at room temperature. The crosshead speed was 50 mm/min, as shown in Figure 2(a). The first run was always disregarded, and the following three loading–unloading cycles were considered. From the displacement–force curve and the picture frame geometry, as shown in Figure 2(b), the shear angle–shear force relation as in Figure 2(c) and, hence, the shear angle–shear stress relation could be determined. Hence, the shear modulus could be calculated from the derivative of the data points on the shear stress versus the radian shear strain plot.

Case Study. ***Experiment description.*** Figure 3 shows the asymmetric form, which was reported previously[16,23] to be used as a benchmark for drapability. The mold contained various combinations of three-dimensional complex features, namely, flat and curved surfaces. The complexity arose from the concave and convex fillets and the curved surfaces of the internal and external radii. Further, the radii had different values and different centers' offsets to determine the dimensional effect. The four internal side curvatures in the mold, denoted by R1, R2, R3, and R4, had radii of 40, 30, 40, and 30 mm, respectively. The offsets of these radii centers out of the mold perimeter were 0, 0, 10, and 10 mm.

It was obvious that the design was not too far from actual practical work pieces, which are adapted in industry, such as in fixation basements. The vacuum-assisted resin infusion (VARI) technique was followed in the sample production, as shown in the schematic of Figure 3(b). The mold was ground, polished, and finally waxed to enhance the surface properties and thus reduce noise induced by the surface roughness. The fibers and mold were then properly vacuum-bagged for VARI. The epoxy was smoothly and slowly allowed to wet and infuse the fabric with the aid of the sucking action of the vacuum. The weight ratio of the Wela supplied epoxy EP2110 to the hardener mix (EH2294/EH2995 = 80:20) was taken, according to the supplier data sheet, to be 100:30. The experiments were carried out on multilayer fabrics, with up to 12 layers, having the same orthogonal directions.

Modeling of the case study. We aimed to evaluate the modeling technique accuracy of the description of the dry fabric draping and to evaluate the capability of the model to predict the wrinkle formation. Therefore, the two previously mentioned modeling methods were carried out to determine the optimum draping strategy, namely, kinematic modeling with Quickform software, developed by the ESI Group, and global deformation modeling with Pamform software. The kinematic concept is based on the advancing front approach, which restricts the deformation within the interfiber shear, and hence, less accurate results are obtained in comparison to the more accurate finite element method (FEM), which considers the fiber mechanical properties.[24]

In the kinematic model, it is only required that one define the initial contact point, direction of draping, preshear of the fabric, critical shear lock angle, and warp/weft directions at the studied point. The mold surface was meshed by visual mesh software with quadrilateral shell elements mostly, except for some meshing sites. The effect of the starting point was studied. The draping simulation trials were applied with different orientations,

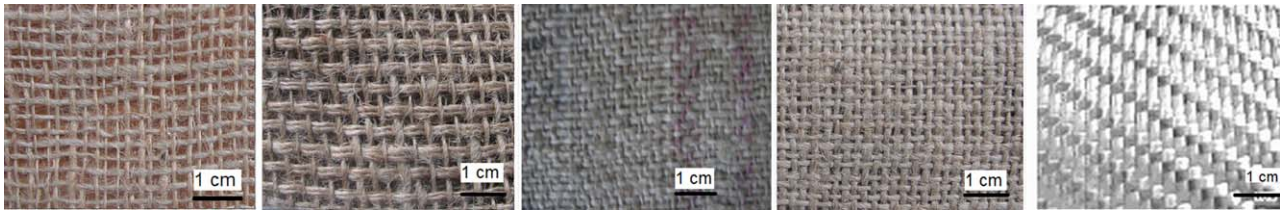

Figure 4. Investigated woven fabrics (from left to right): JFEN 1 × 1, JFEN 2 × 1, JFEK 1 × 1, JFGN 1 × 1, and GFG. [Color figure can be viewed in the online issue, which is available at wileyonlinelibrary.com.]

Table II. Physical and Mechanical Results of the Characterization Tests

Fabric type	JFEN 1 × 1				JFEN 2 × 1				JFEK 1 × 1				JFGN 1 × 1			
Property	*M*	SD			*M*	SD			*M*	SD			*M*	SD		
Areal density (g/m^2)	228.9	3.5			513.9	55.0			765.6	3.3			374.0	5.2		
	Warp	SD	Weft	SD	Warp	SD	Weft	SD	Warp	SD	Weft	SD	Warp	SD	Weft	SD
Thread count (ends/in.)	8	0.2	9	0.2	5.8	0.13	8	0.09	9.4	0.2	12.5	0.5	11.4	0.14	11.6	0.14
Diameter (μm)	0.72	0.08	0.66	0.1	0.75	0.3	0.85	0.12	1.8	0.1	1.32	0.1	1.0	0.1	0.9	0.05
Yarn (Tex)	244.7	14.5	241.0	17.4	304.8	35.6	748.6	129.8	1349.8	509.3	528.6	9.9	465.0	19.1	368.0	48.8
Strength (cN/Tex)[a]	14.7	1.6	10.1	4.2	15.3	2.2	8.9	1.9	6.5	1.2	8.7	3.1	10.2	1.5	12.6	5.1
Strain (%)	1.29	0.14	1.18	0.33	1.2	0.41	1.7	0.29	1.52	0.407	1.19	0.3	1.36	0.11	1.09	0.24
Maximum force (N)[b]	301.0	40.8	164.5	8.0	375.8	86.1	892.6	201.0	885.2	384.8	889.4	151.1	585.6	302.3	788.1	146.4
Cover factor	5.00		5.58		4.05		8.75		13.81		11.49		9.83		8.90	
Flexural rigidity (g cm)[26]	1.45		1.35		1.75		0.85		1.40		1.20		4.20		4.00	
Bending stiffness (MPa)	0.00030		0.00029		0.00037		0.00018		0.00005		0.00004		0.00090		0.00086	
Tensile stiffness (MPa)	41.2	3.3	19.5	1.1	17.5	2.49	16.4	0.9	13.0	1.2	12.7	1.0	17.3	1.1	19.7	3.3
G (MPa)	0.0363												0.064			
Lock angle (°)	35.9												22.4			

M, mean; SD, standard deviation.

[a] DIN EN 13895-1.

[b] DIN EN ISO 13934.

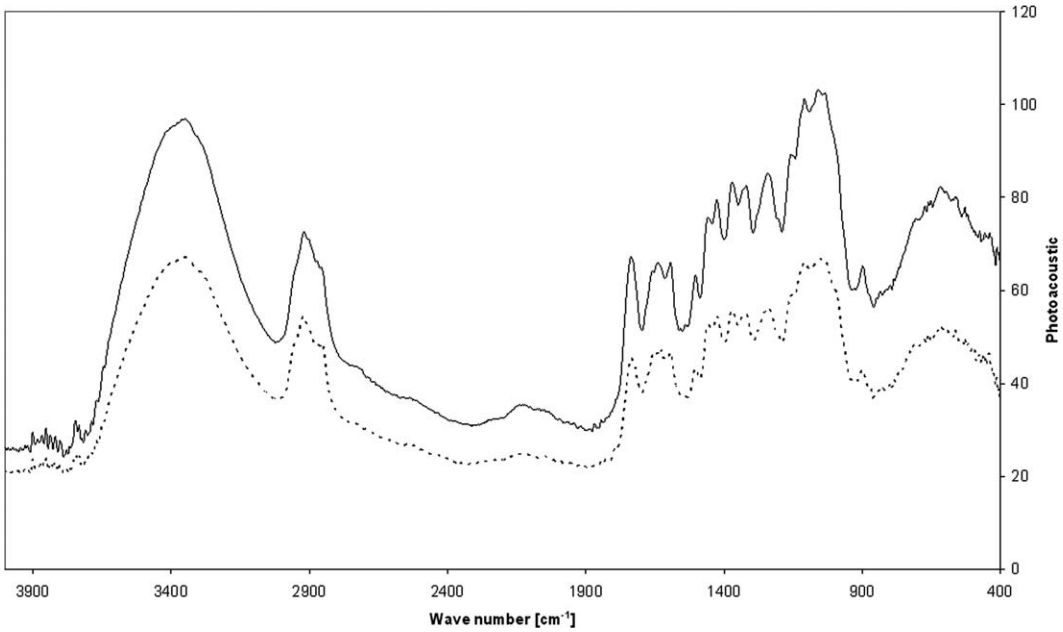

Figure 5. FTIR analysis of the Egyptian and German jute fabrics.

namely, the warp and the 45° biased directions. The constraints with the lowest shear-angle critical zone, especially at the fillets, which were more likely to have a bridging problem, were further used in the practical experiment.

In the global deformation model, the material characterization of the fabric tensile modulus in both orthogonal directions, the bending modulus with the Shirley tester, the in-plane G with the picture frame, and the coefficient of friction in the case of multiple layers were studied. The coefficient of friction was roughly estimated from the literature[25] as 0.4. The underlying form, blank holder, and stamp geometries were defined.

Afterward, the draped fabric was impregnated by resin *in vacuo*. The drapability of the jute fabrics was then evaluated on the basis of direct measurement for the product geometrical features after impregnation with resin. The measured dimensions were then compared with the original underlying dimensions of the mold. The resin impregnation was not modeled in this study because the available model deals with the macroflow of resin around the fibers. This matched the case of synthetic fibers and not the microflow within the fibers themselves. Modeling was performed with tension applied by blank holders. The same procedure was done in the experimental part, where blank holders were used during draping and resin impregnation until approximate curing.

RESULTS

Physical Properties

Figure 4 shows the investigated woven fabrics, whereas Table II summarizes the results of the geometrical, physical, and mechanical testing. In some cases, measurements in the warp and weft directions showed that the yarns used significantly varied around the average diameter. The yarn diameters and Tex numbers in both the warp and weft directions were consistent for jute fibre Egypt thin (JFEN) 1 × 1 and jute fibre germany thin (JFGN) 1 × 1 (homogeneous 0/90 fabrics); this resulted in equivalent values of linear density in both directions. The linear

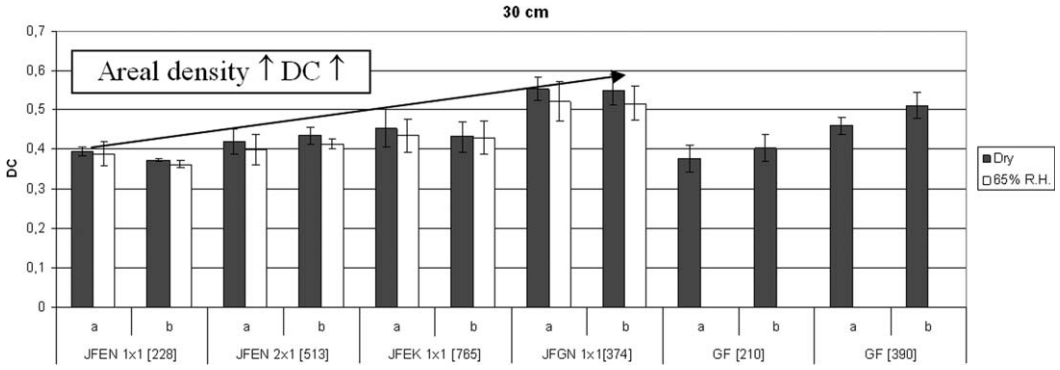

Figure 6. DC for various jute- and glass-fiber woven fabrics under ambient conditions cut at a diameter of 30 cm (the planar density in grams per square meter is between brackets).

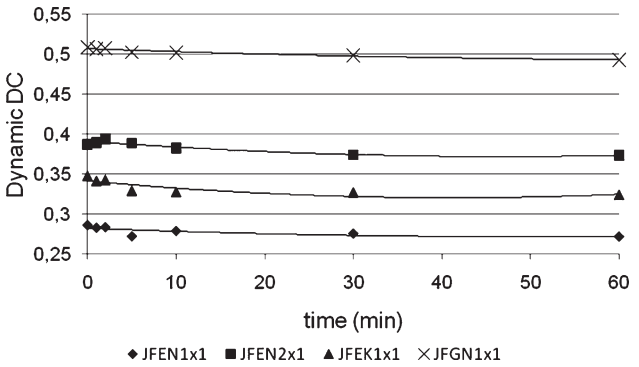

Figure 7. DC for various jute-fiber fabrics cut at a diameter of 36 cm and tested under ambient humidity.

density or Tex number depicts the resistance of the fabric to bending and conformation to the underlying surface. Similarly, the areal density is an important property in defining the fabric type and indicates its suitability for draping. Considering the results listed in Table III, one can predict that the draping behavior was best for JFEN 1 × 1, followed by jute fibre Egypt thick (JFEK) 1 × 1, and further the JFEN 2 × 1 and JFEK 1 × 1 fabrics. Generally, the comparable JFEN 1 × 1 and JFGN 1 × 1 results would denote similar draping characteristics, although the thread count (number of yarns per unit length) showed a slight unevenness in the warp and weft directions for the JFEN 1 × 1 fabrics compared to the JFGN 1 × 1 ones.

With regard to the tensile behavior, we observed that the yarn strength was not proportional to the textile maximum strength values, and this was attributed to the difference in the thread counts among the fabrics. The modeling parameters derived from the Shirley tester, picture frame, and tensile testing, namely the flexural rigidity, G, and E_1 and E_2, are also listed in Table II. The modeling parameters were characterized only for two types of similar areal density fabrics representing the Egyptian and German fabric supplies.

FTIR Analysis

Figure 5 illustrates the FTIR analysis of both the Egyptian and German jute fabrics. The main peaks found were as follows. The peak at 3350 cm^{-1} corresponded to the free hydroxyl group.[7] The peak at 1736 cm^{-1}, which corresponded to C═O stretching vibrations, suggested the existence of carboxylic/ester groups. The presence of lignin was detected by the peaks at 1450, 1050, 887, and 817 cm^{-1}. The band at 817 cm^{-1} appeared as a shoulder, and it arose when pectin and fats were removed.[7] Another change was observed with the diminishing of the C═C vibration group at 1516 cm^{-1} when instauration in oil traces and fatty substances was removed. The results indicate that both curves were similar to each other, and the measured peaks were found in both types of jutes. Hence, no difference from chemical treatment or preparation was expected. This eliminated the fiber composition and/or treatment/structure from as a reason for the deviated draping behavior.

Draping Behavior Characterization

A low DC implies easy deformation, whereas an increase in the coefficient value describes a more stiff fiber that is less vulnerable to deformation. Applying the aforementioned procedures for both the jute- and glass-fiber fabrics under ambient humidity conditions rendered the results illustrated in Figure 6 for the sample 30 cm in diameter.

The most significant result was that JFEN 1 × 1 and GF210 had comparable DC values in addition to their close areal densities; this is a promising result for natural-fiber applications. Shyr[27] tested four natural-fiber fabrics at 65% RH and reported that the DCs of cotton (148.7 g/m^2), flax (189.4 g/m^2), silk (98.9 g/m^2), and wool (200.5 g/m^2) were around 0.52, 0.43, 0.28, and 0.37, respectively. Because the jute fabric used in this study had a slightly higher areal density of 229 g/m^2, a DC of 0.38 for the JFEN 1 × 1 was comparable to values reported in the literature under similar conditions; this suggests a good draping behavior.

Although the areal densities of JFGN 1 × 1 (374 g/m^2) was lower than that of JFEN 2 × 1 (513 g/m^2), it had a higher DC (lower drapability), which could be attributed to the greater number of threads per unit length, as indicated by the thread count values (11.4 and 5.8, respectively).

Taking Figures 6 and 7 into consideration, we observed that an increase in RH decreased DC, and hence, the drapability was

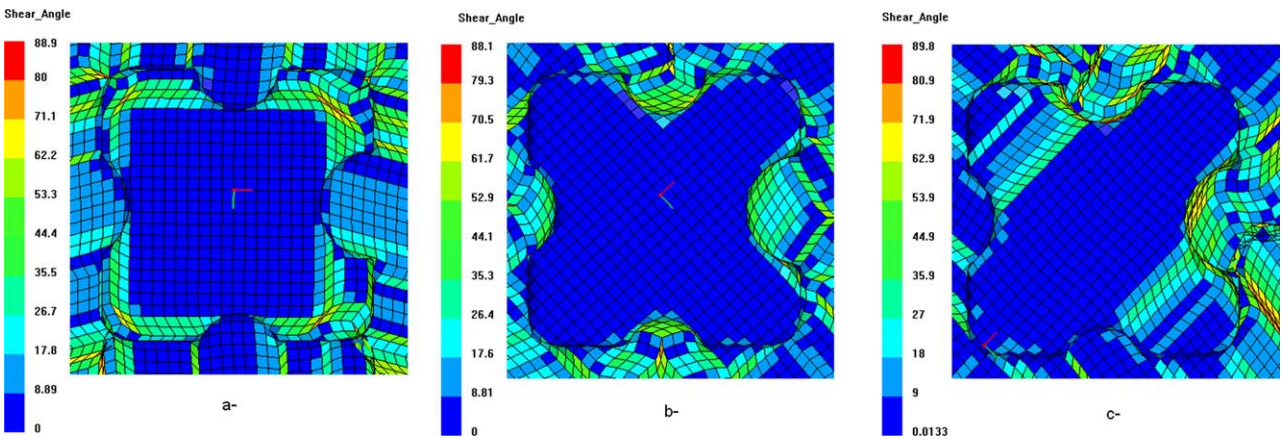

Figure 8. Effect of the draping direction on the shear angle zones: (a) 0° (middle-point start), (b) 45° (middle-point start), and (c) 45° (the start was not in the middle). [Color figure can be viewed in the online issue, which is available at wileyonlinelibrary.com.]

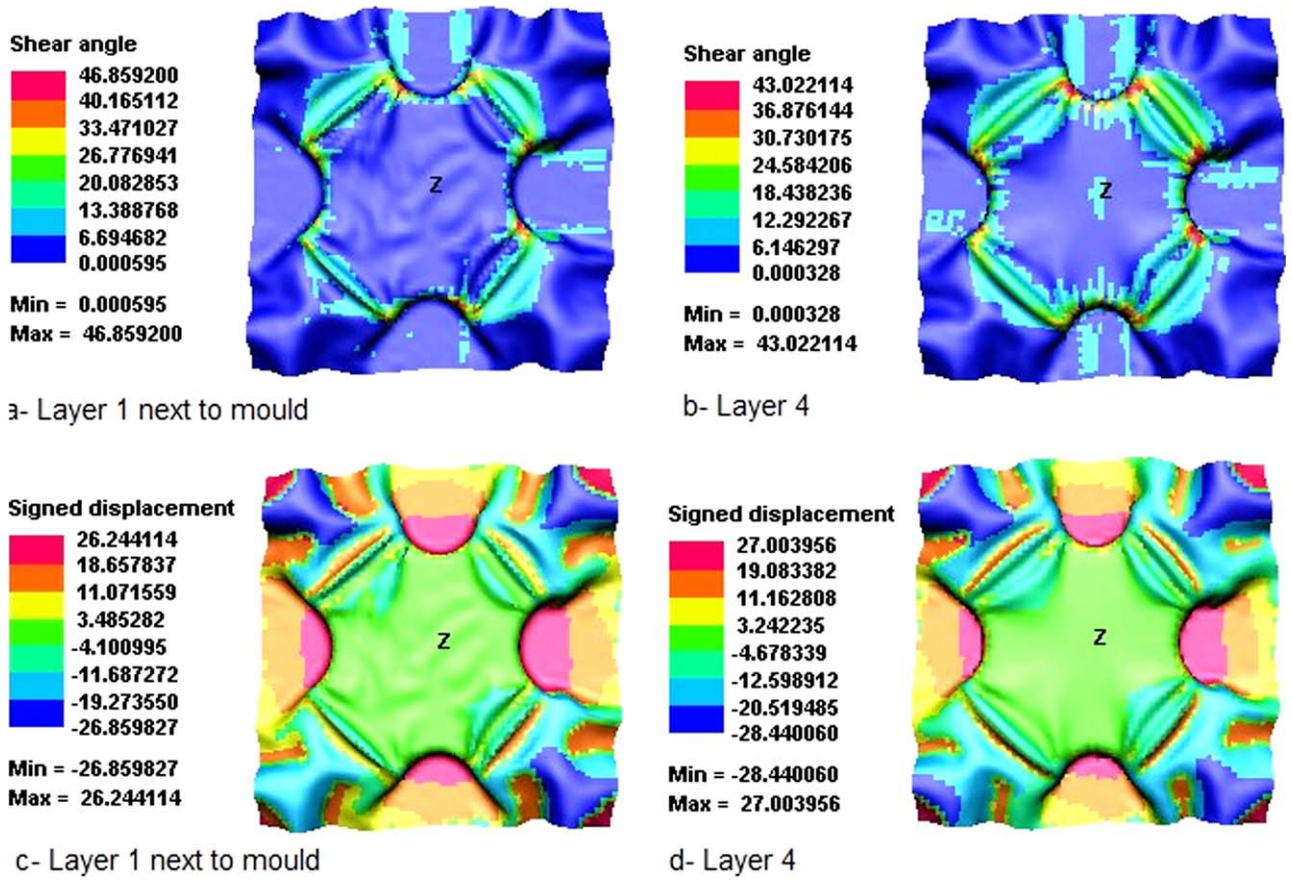

Figure 9. Pamform model of the jute fabric: (a) shear angle and (b) signed kinematic displacement. [Color figure can be viewed in the online issue, which is available at wileyonlinelibrary.com.]

improved by 5–10%. However, the humidity could not be infinitely increased during composite processing, where moist fabrics need to be avoided to prevent bubbles and thus void formation within the final product, especially where resin curing is achieved at elevated temperatures.

Figure 7 represents the change in DC with time, where the DC was observed to decrease slightly with elapsing time. However, the DC tended to stabilize after around 30–60 min, depending on the sample areal density and weaving texture. Again, this was expected because of the longer influence of gravitational forces accompanied by continuous slippage between the warp and weft yarns until the yarn stiffness holding the fabric upward resisted the downward movement of gravity. These observations were broader than those observed by Jeong,[28] where he limited the test time span to 10 min; this study was prolonged to 60 min. As shown in Figure 7, some fabrics, such as JFGN 1 × 1, attained their steady-state situation first after 60 min. However, the logarithmic decrease of DC with time remained similar to that reported by Jeong.[28]

A correlation between the DC values and the bending stiffness was investigated and found in the literature.[29] In addition, we needed to implement the measured DC value in the commercial modeling software instead of many values considering the tensile, shear, and bending stiffness.

Case Study: Drapability over an Asymmetric Form

Modeling Results. Figure 8 illustrates the shear zones at different draping directions and different starting points. Only three cases are given in Figure 7 for the sake of demonstration. A biased direction was selected from the simulation trials because of the lowest value of the critical shear angle zones (Figure 8). The simulation study showed that the contact point, at the middle of the upper surface, such as that in Figure 8(a,b), guaranteed the shortest way for a yarn. On the other side, the offset from the midpoint, as shown in Figure 8(c), induced more critical shear zones. According to ref. [16], surfaces with no concave radii, such as the upper surface and the upper fillets, should have been the first to drape. Then, the convex radii sites were draped next because they were characterized with their out-of-plane curvatures and their greater affinity to have bridging. The critical shear angle areas were handled with suitable tool geometry as advised previously.[16] The configuration shown in Figure 8(c) was disregarded because it was out of the midpoint. The configuration shown in Figure 8(b) suffered from high-shear zones at the fillet radii in the inner curvatures. Therefore, the configuration shown in Figure 8(a) was selected for the experimental study. A kinematic approach helped to provide a rough estimation of the draping strategy. However, the wrinkles were not detected by this kinematic approach.

Figure 10. Case study experiment: (a) VARI system of the mold and (b) measured radii of the dismounted samples. [Color figure can be viewed in the online issue, which is available at wileyonlinelibrary.com.]

With the global deformation modeling, the wrinkling sites could be estimated. Figure 9 shows the shear angle exceeding the lock angle of 22.4°. Wrinkles were noticeable after the modeling of the draping stage. The resin infusion *in vacuo* was not modeled, as previously mentioned. The blank holding process was represented by four stamps located at the four inner curvatures. Therefore, the fabric draping at the external curvatures was not considered in the model, although manual draping was applied in the experimental work. The four stamps applied tensile stress between every two consequent curvatures. These sites were characterized with high shearing, as shown in Figure 9(a). The maximum shearing zone was located between the complete semicircles more than between the offset circles. The wrinkling sites could also be depicted through the signed kinematic displacement chart shown in Figure 9(c). The change in color in Figure 9(c) shows the alteration of the kinematic displacement sign, which indicated the likely formation of wrinkles at these sites. The maximum altering was again in the same site of maximum shearing.

In a comparison of the behavior of the first layer next to the mold [Figure 9(a,c)] with respect to the fourth one [Figure 9(b,d)], we found that local wrinkling sites were found at the middle of the fabric, and these wrinkles were missing on the fourth one. Shearing was slightly decreased in the fourth layer [Figure 9(b)] in comparison to that of the layer next to the mold [Figure 9(a)], similar to the kinematic signed strain, as shown in Figure 9(b,d). This could be explained in terms of the friction coefficient between layers. Blank holders applied stretching tensile stress on the in-contact fourth layer. The stress was transferred to the first layer next to the mold but after being reduced from one layer to another because of the friction coefficient.

Experimental Results. The JFGN 1 × 1 fabric, which was characterized by its relatively high DC and thus low drapability, was selected for this case study. The complex mold, as determined from the kinematic model approach, was impregnated with resin from the top center to ensure short path infiltration in all directions, as illustrated in Figure 10(a). Vacuum suction was carried out around the perimeter of the mold. The draping efficiency was investigated in terms of an accurate reproduction of the mold dimensions. Thus, radii/fillets were mechanically measured at the points indicated in Figure 10(b). The final product was inspected further for any wrinkling sites.

Figure 11 illustrates the composite series produced with the same setup with various multilayer assemblies of the JFGN 1 × 1 fabric. In all cases, impregnation was found to be complete, and no resin-starved spots were observed. Generally speaking, the draping behavior was acceptable, and all geometrical features were verified. We noted that with an increased number of fabric layers (>4), wrinkles were clearly observed, especially at the upper surfaces of the product. Kinematic modeling failed to detect the wrinkle formation with the given geometry and fabric shearing properties. The global deformation predicted the wrinkling at any number of layers greater than one layer. This could be explained according to the following:

- The description of the boundary conditions, given the blank holders, the vacuum application, and the consequent compaction effect on the fabric layers, was insufficient.
- The impregnating resin was believed to induce an upthrust force between the layers, which reduced the resistance to fabric draping.

However, this gave us the idea that the experimental results were closer to those of the global deformation model.

Wrinkles were most clearly be depicted, as shown in Figure 12(a), in the case of the composite composed of 12 layers of jute woven fabric. The zone of wrinkle formation was between the half-circles, where the blank holders asserted tensile forces upon the fabric textile. This induced in-plane orthogonal

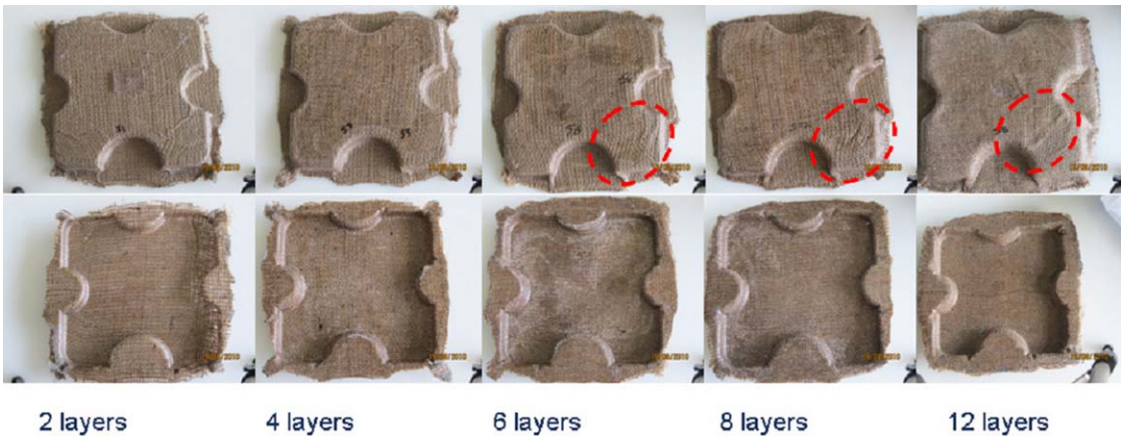

Figure 11. Multiple layers draped and resin-infused over the complex mold. [Color figure can be viewed in the online issue, which is available at wileyonlinelibrary.com.]

compressive stress. Because the bending stiffness was much lower than the in-plane stiffness, as shown in Table II, this compression stress was converted to an out-of-plane deformation or wrinkle.[18] According to Boisse et al.,[18] these wrinkles appeared because of the lower energy dissipation in comparison to the in-plane dissipation.

Under the same conditions and for the sake of comparing the jute-fiber draping behavior with the glass-fiber draping behavior, the use of 12 layers of GF390 glass fibers also rendered clearly identifiable wrinkles at the same position, as shown in Figure 12(b).

The fillet radii labeled in Figure 10(b) were measured at their bottom side (which was in direct contact with the mold surface), as shown in Figure 13(a). The fillet radii in the final composite product suffered from a bridging problem, as schematically illustrated in Figure 13(b). The bridging phenomenon primarily took place when the fabric was laid over a concave surface. When the applied vacuum was not sufficient to tightly force the fabric onto the die, in addition to the fabric ends being subjected to stretching during the lamination procedure, bridging was highly promoted. Moreover, during resin transfer, normal stresses developed, and this led to a forcing of the fiber away from the mold. This further accentuated the bridging phenomenon. To overcome such a problem, a compromise is required between the blank holder force and the force generated by the vacuum to make the fabric conform to the mold concave curvature. A higher stretching force due to blank holding will overcome the force generated by the vacuum, and on the other hand, less force may allow the resin to push the fabric away during the resin flow.

For the undersized edge fillets (i.e., relative to fabric thickness or multilayered laminates), fillet sizes larger than the nominal dimensions were observed [Figure 13(c)]; this led to an aspect to be taken into consideration in product design and a tool for certain fabric characteristics.

As depicted in Figure 13(d), the deviations from the reference radius dimensions increased with the application of a greater

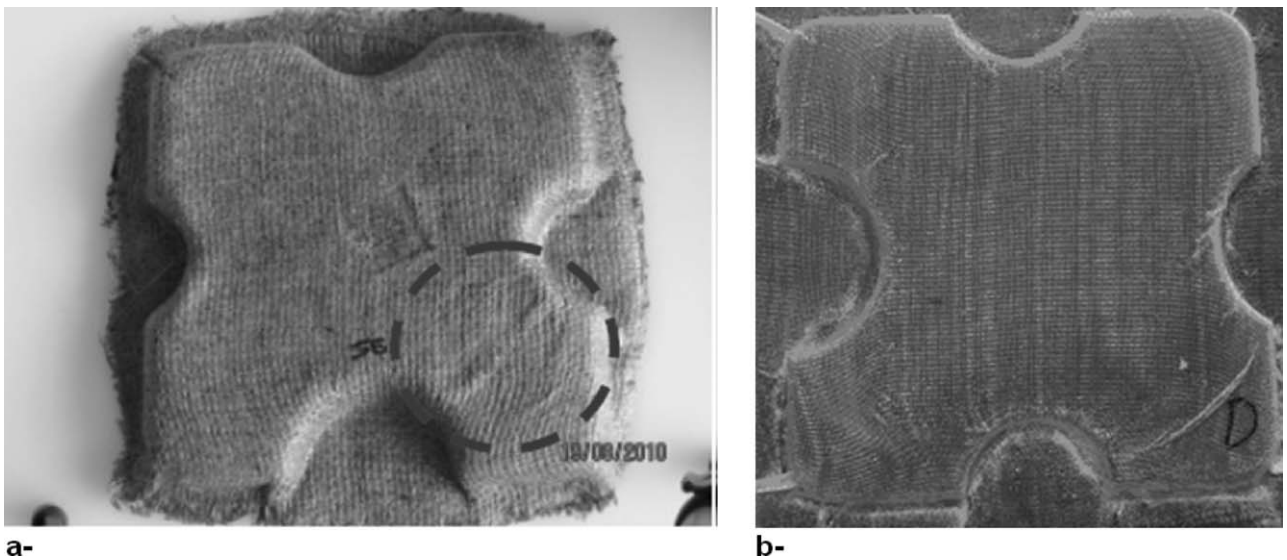

Figure 12. Draped jute-fiber woven fabric after VARI showing wrinkling sites: (a) JFGN1 × 1 and (b) GF390.

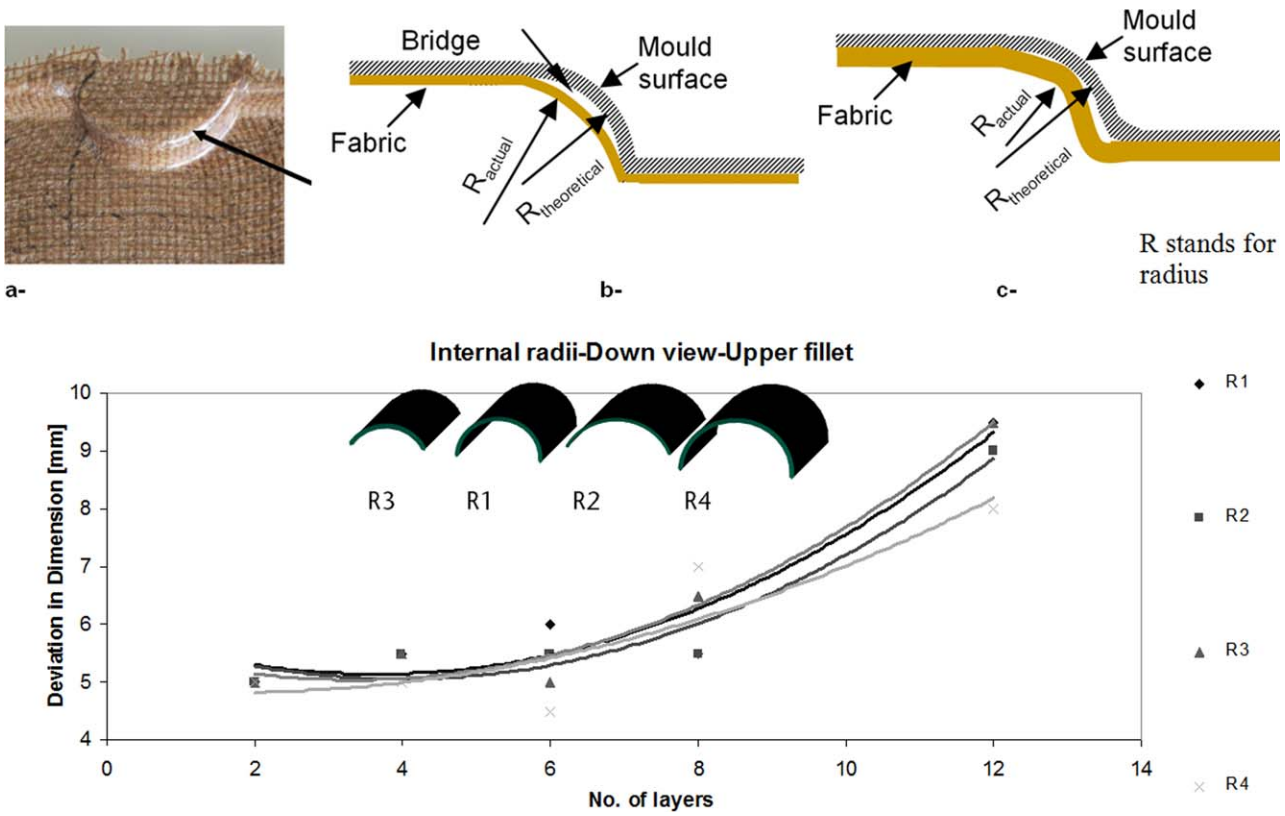

Figure 13. Measured check radii of the asymmetric form. [Color figure can be viewed in the online issue, which is available at wileyonlinelibrary.com.]

number of fabric layers. The curvatures of greater diameters (R2 and R4) resulted in lower deviations. It is also worth noting that off-centered curvatures (R2 and R3) were found to affect the geometrical conformance. As indicated by Figure 13(d), the deviations were greater with smaller fillets and where there was an offset in the center.

CONCLUSIONS

The characterization of jute fabrics with different weaving structures and suppliers was carried out. The required properties were defined with further modeling. The jute-fiber fabrics had promising DC values, which were comparable with those of common glass-fiber fabrics with similar plain woven structures and areal densities. The DC values were generally proportional to the fabric areal density but were further affected by the thread count and yarn stiffness. DC decreased with increased relative humidity, and this led to improved draping behavior. Kinematic modeling helped in the quick determination of an acceptable draping strategy but not in diagnosing problems such as wrinkle formation. On the other hand, global deformation modeling helps in the explanation of the wrinkle formation. The case study of a complex asymmetric form proved similar behavior in the jute- and glass-fiber fabrics under resin-transfer processing. In both cases, an increase in the layer number during composite molding led to greater deviations from the design/mold dimensions. These were further found to increase the reduced fillet size and increased center offset.

ACKNOWLEDGMENTS

The authors thank the Egyptian and German funding associations german Egyptian scientific projects (GESP) and deutscher akademischer austauschdienst (DAAD) through projects 50016808 and 51241598. The discussions with G. Ziegmann and L. Steuernagel were also helpful. The work of colleagues and students S. Reich, M. Hegazy, Y. Abdin, M. El-Zohairy, and M. Giese is much appreciated.

REFERENCES

1. Bledzki, A. K.; Sperber, V. E.; Faruk, O. *Rapra Rev. Rep.* **2002**, 13, Report 152.
2. Bogoeva-Gaceva, G.; Avella, M.; Malinconico, M.; Buzarovska, A.; Grozdanov, A.; Gentile, G.; Errico, M. *Polym. Compos.* **2007**, *28*, 98.
3. Taha, I.; Steuernagel, L.; Ziegmann, G. *Compos. Interface* **2007**, *14*, 669.
4. Bos, H.; Muessig, J.; Van den Oever, J. *Compos. A* **2006**, *37*, 1591.
5. Taha, I.; El-Sabbagh, A.; Ziegmann, G. *Polym. Polym. Compos.* **2008**, *16*, 295.
6. Moran, J.; Alvarez, V.; Petrucci, R.; Kenny, J.; Vazquez, A. J. *Appl. Polym. Sci.* **2007**, *103*, 228.
7. El-Sabbagh, A.; Steuernagel, L.; Ziegmann, G. J. *Appl. Polym. Sci.* **2009**, *111*, 2279.

8. Patel, B.; Acharya, S.; Mishra, D. *Int. J. Eng. Sci. Technol.* **2011**, *3*, 213.
9. Ahmed, A.; Vijayarangan, S.; Rajput, C. J. *Reinf. Plast. Compos.* **2006**, *25*, 1549.
10. Ray, D.; Bose, N.; Mohanty, A.; Misra, M. *Compos. B* **2007**, *38*, 380.
11. Rowell, R.; O'Dell, J.; Basak, R.; Sarkar, M. In International Seminar on Jute and Allied Fibres: Changing Global Scenario; Nirjaft: Calcutta, **1998**.
12. Collier, B. *Cloth. Text. Res. J.* **1991**, *10*, 46.
13. Pierce, F. J. *Text. Inst.* **1930**, *21*, 377.
14. Kankare, N.; May-Plumlee, T. *Int. J. Cloth. Sci. Technol.* **2005**, *17*, 109.
15. Chu, C.; Cummings, C.; Teixeira, N. *Text. Res. J.* **1950**, *20*, 539.
16. Hancock, S.; Potter, K. *Compos. A* **2006**, *37*, 413.
17. Lin, H.; Wang, J.; Long, A.; Clifford, M.; Harrison, P. *Compos. Sci. Technol.* **2007**, *67*, 3242.
18. Boisse, P.; Hamila, N.; Vidal-Salle, E.; Dumont, F. *Compos. Sci. Technol.* **2011**, *71*, 683.
19. Fong, L.; Advani, S. In Proceedings of the American Society for Composites 9th Technical Conference; Technomic: Lancaster, PA, **1994**.
20. Ramzy, A. M.S. Thesis, Clausthal University of Technology, **2011**.
21. Jer-Yan, L.; Pin-Ning, W.; Tien-Wei, S. *Text. Res. J.* **2008**, *78*, 911.
22. Kokas-Palicska, L.; Szuecs, I.; Borka, Z. *Acta Polytech. Hung.* **2008**, *5*, 75.
23. Potter, K. *Compos. A* **2002**, *33*, 677.
24. Vanclooster, K.; Lomov, S.; Verpoest, I. *Int. J. Mater. Form.* **2008**, *1*, 961.
25. Roul, C. International Jute Commodity System; Northern Book Centre: New Delhi, **2009**.
26. Abdin, Y. M.S. Thesis, Ain Shams University, **2011**.
27. Shyr, T.; Wang, P.; Cheng, K. *Fibres Text. East Eur.* **2007**, *15*, 81.
28. Jeong, Y. J. *Text. Inst.* **1998**, *89*, 59.
29. Morooka, H.; Masako, N. J. *Text. Machin. Soc. Jpn.* **1976**, *22*, 67.